Wind Regimes in Southern California Winter

S. Conil,[1,2] A. Hall,[1] and M. Ghil[1,2,3]

Two different and complementary classification methods are applied to the daily mean 10-m wind simulated by the MM5 mesoscale atmospheric model during the 1995–2003 winter seasons. The MM5 model is implemented on a triply nested grid with increasing resolutions of 54/18/6 km that covers the Western United States, with greatest detail over the Southern California region. Both classification methods indicate that the atmospheric variability during winter is dominated by three robust wind regimes. The first regime describes a strong northeasterly flow over the Los Angeles Basin and can be identified with Santa Ana conditions. The second regime is a moderate northwesterly flow over the ocean with a maximum in the Southern California Bight. The third regime shows a stronger northwesterly wind, shifted southward and with a maximum near Point Conception. These last two patterns are slight variants of the climatological mean winds. The large-scale synoptic conditions associated with each local wind regime bear no relationship with any of the large-scale weather regimes that characterize the North Pacific/North American sector.

1. Introduction

During Southern California fall, winter and early spring, the mean winds are weaker than during the summer, but they are subject to much higher variability. These wind variations are known to have large impacts on ocean dynamics and biology (Hu and Liu, 2003; Travisña et al., 2003). They also have a strong influence on the air quality of this highly urbanized region (Lu et al., 2003). During the fall, the wind variability is particularly critical for the development and evolution of wild fires (Westerling et al., 2004).

The typical Southern California winter surface circulation is dominated by a moderate along-shore wind over the ocean blowing from the northwest at 4–4.5 ms^{-1} Winant and Dorman (1997) have shown that the intensity of this NW wind is highly variable and that most of its fluctuations are spatially homogeneous over the Southern California Bight. These variations are commonly thought to be controlled by the changes of the intensity or the position of the high-pressure center located off the Cali-

[1]Department of Atmospheric and Oceanic Sciences, UCLA, Los Angeles, California, USA
[2]Institute of Geophysics and Planetary Physics, UCLA, Los Angeles, California, USA
[3]Additional affiliation: Département Terre-Atmosphère-Océan, and Laboratoire de Météorologie Dynamique du CNRS/IPSL, Ecole Normale Supérieure, Paris, FRANCE

0094-8276/04/$5.00

fornia coast.

This typical situation is often perturbed by a synoptic regime characterized by a high-pressure pattern centered over the Great Basin, northeast of Southern California. This regime, commonly named Santa Ana, is characterized by strong offshore winds with little diurnal variation and low relative humidities. During a typical Santa Ana event, the winds blow from the northeast and they are particularly strong over the Los Angeles Basin and over the slopes of the mountain ranges of Northern Baja California.

In this paper we characterize more precisely the wind variability over Southern California by defining the major wind regimes using two distinct classification methods. Since a comprehensive view of these regimes has been missing up till now, our goal is to describe the local circulation and the synoptic conditions associated with these regimes.

2. Numerical Simulation and Data Analysis

No observational dataset with sufficient spatio-temporal resolution exists to allow the description we aim for. Hence we performed a high-resolution simulation of the regional climate with the mesoscale model MM5 to have a realistic representation of the complex topography and coastlines of Southern California. Three nested grids of resolution 54/18/6 km were implemented covering the Western United States (32N–39N; 125W–113W) and zooming in on Southern California. The initial atmospheric states and the lateral and lower boundary conditions were derived from the Eta analysis for the period starting 1 January 1995 and ending 31 December 2003. The Eta forcing data were obtained through NCAR's GCIP Model Output Archive and have a nominal horizontal grid resolution of 40 km. The lateral conditions were updated every 3 hours. In addition to the model simulation we also used the NCEP daily reanalysis over the same period.

From the 9-year hourly model outputs we computed the daily mean anomalies from a composite seasonal cycle during the winter season, from October to March. We use daily averages of the wind to remove the influence of the local diurnal circulation(land/sea breeze and diurnal mountain winds). Figure 1 shows the mean wind simulated by the model's innermost 6 km-resolution domain in winter, as well as the standard deviation of the wind speed anomalies. The orientation and the magnitude of the winds over the ocean are well simulated when compared to buoy observations (Winant and Dorman, 1997). In the Mojave and Sonoran desert region, the 10-m winds are weaker than over the ocean but are also blowing toward the southeast. In the Los Angeles area the mean winds are northeasterly, mainly because of the strong winds blowing during the intermittent Santa Ana events.

The intraseasonal-to-interannual wind variability is largest over the ocean. Buoy observations suggest that this variability is larger than the seasonal cycle (Winant and Dorman, 1997), and our simulations confirm this fact. The wind variance is also strong over the slopes of the Tehachapi Moutains and the Laguna Mountains east of Los Angeles, as well as over the complex low-lying topography north of the Los Angeles Basin. From Los

Angeles to San Diego, between the coast and the coastal mountain range, the mean wind as well as its variability are very weak.

To describe the coherent spatial structures of the wind variability, we computed empirical orthogonal functions (EOFs) of the wind anomalies (Ludwig et al., 2004). The direction ambiguity inherent in complex EOFs led to results that were difficult to interpret. Hence we used the real-vector method of Kaihatu et al. (1998). We have also computed the EOF modes of the surface pressure anomalies (see Fig. 2). The wind EOFs were computed over the innermost 6-km resolution domain shown in Fig. 1, while the surface pressure EOF modes were computed over the outermost 54-km resolution domain.

The wind variability is dominated by two distinct modes that each represents 39% and 32% of the variance. The first EOF of surface pressure anomalies acounts for 78% of the variance. The second surface pressure mode is also well separated from the third and represents 14% of the variance. The two leading modes of surface pressure (in the outermost domain) and wind (in the innermost domain) are closely connected pairwise: the correlation reaches 0.73 for the first pair and 0.88 for the second.

The first mode of variability is characterized by a surface pressure increase throughout the domain, with a maximum over the Great Basin. The corresponding wind anomalies are dominated by strong northeasterlies blowing from the Great Basin into the Los Angeles Basin and over the ocean. The second mode of variability is dominated by an East–West pressure dipole, with an increase over the eastern part of the domain and a decrease over the ocean and the coast. The corresponding wind anomalies are strong north-northwesterlies over the entire domain, but are particularly strong over the ocean. They are geostrophically related to the pressure pattern.

3. Multiple Wind Regimes

The EOF analysis is linear and hence the signs and amplitudes of the patterns in Fig. 2 are arbitrary. But in reality the dry northeasterly Santa Ana pattern is much more common than the opposing wet southwesterly regime (a fact not apparent from the EOF analysis alone). It is thus essential to define the wind regimes in a nonlinear and sign-dependent fashion. We achieve this by using two distinct and independent classification techniques. One method is the k-means algorithm of Michelangeli et al. (1995) and the other is the probabilistic clustering scheme of Smyth et al. (1999), based on finite mixture models.

These two schemes were applied to a range of leading wind EOF modes (from 2 to 8) and for a range of clusters (from 2 to 8). The two classification methods give an optimal number of clusters somewhere between 3 and 5. The best agreement between the two methods was found using the 2 first EOFs classified in 3 clusters. We carefully verified that these results are insensitive to clustering parameters or the domain of the analysis. We present the results of the mixture model clustering because it has several advantages compared to the k-means scheme, which was merely used as an independent verification of the results (Kondrashov et al., 2004). Each regime is defined by an ellipse centered on the mode of

a gaussian component and with semi-axes equal to 1.5 times the standard deviation in each principal direction.

The three dominant wind regimes during Southern California winter are shown in Fig. 3. The first regime is typical of Santa Ana conditions with strong northeasterlies (reaching 8 $m.s^{-1}$) over the Los Angeles Basin and Baja California. Over the ocean, these winds are also blowing from the northeast but are much weaker. Cluster 1 contains 13% of the 1274 days used in this analysis. Strong winds are also found on the western slopes of the Sierra Nevada mountains, in northwestern Baja California and over the Gulf of California (not shown).

Regimes 2 and 3 are very similar to the climatological mean wind, particularly over the ocean. In Regime 2 the wind speed is weaker and the wind direction is shifted eastward. Almost 27% of the 1274 days belong to this regime. The third regime is characterized by an intensification of the northwesterlies over the ocean just off Point Conception. This regime represents 42% of the days. A fraction of 18% of the days are not classified because they are not close enough to the centroids of any of these three major clusters.

The average duration of a Santa Ana event is 1.7 days, with a standard deviation of 1 day. This typical duration is roughly consistent with the one estimated by Raphael (2003), based on large-scale observations. Regimes 2 and 3 have a mean duration of 1.6 and 2.4 days, respectively, with standard deviations of 1.1 and 2 days. Very few Santa Ana events last more than 3 days (only 5 events last between 4 and 6 days). By contrast, 39 events in Regime 3 (17% of the total) last 4–9 days. While Regime 3 occurs more frequently at the beginning (October, November) and end (March) of the winter period, Regime 2 is slightly more frequent in the late winter (January, February and March). As noticed by Raphael (2003), the occurrence peak of the Santa Ana regime is in early winter (November and December).

The large-scale synoptic conditions over the North Pacific and western North America associated with the 3 dominant wind regimes are shown in Fig. 4. The climatological sea level pressure (SLP) for the extended winter (Oct.-Mar.) is also displayed for reference. The Santa Ana regime occurs simultaneously with the onset of a strong high-pressure centered over the Great Basin (Sommers, 1978). The Great Basin high is generally thought to appear in conjunction with a low-pressure system off the coast of California (Raphael, 2003). This is not the case, however, in our analysis, where the Great Basin high alone favors the occurrence of the Santa Ana regime. On the other hand, Regime 2 is linearly associated with a slight deepening and shift of the Aleutian Low and a decrease of the surface pressure over the Great Basin. Wind regime 3 is not associated with any significant large-scale SLP anomalies, hence it can be thought of as corresponding to the mean state of the large-scale circulation.

The North Pacific/North American climate experiences strong intraseasonal and interannual variability. This variability is dominated by a few weather regimes. It is believed that these weather regimes have a strong impact on the local climate of the western United States and California in particular (Robertson and Ghil, 1999; Leung et al., 2003). We have investigated therefore the relationships between these large-scale weather regimes of the North Pacific/North American region and the local wind regimes shown in Fig. 3. We identified the

large-scale regimes by applying mixture model clustering to the 500-hPa geopotential height winter anomalies over the same interval (1995–2003). Using the NCEP reanalysis heights, we found 4 or 6 regimes to be significant. The four most salient regimes correspond mostly to the two opposite but asymmetrical phases of the North Pacific/American and Western Pacific teleconnections. Surprisingly, each local regime is about equally likely to occur under any of the large-scale weather regimes. During none of these large-scale weather regimes has any impact on either the probability of occurrence or the duration of the local regimes.

4. Concluding Remarks

The surface winds of Southern California are highly variable during winter. These wind changes are particularly strong over the coastal ocean and the Los Angeles Basin. We have shown that these variations are organized into three well defined and coherent wind regimes. The Santa Ana regime is characterized by strong wind blowing from the northeast over the Los Angeles Basin and the Santa Monica Bight. The two other regimes describe weaker and stronger northwesterlies over the ocean and are also associated with slight shifts in direction.

No significant correlation was found between the local wind regimes and the large-scale dominant weather regimes of the North Pacific/North American sector. Apparently, the synoptic conditions that favored the Santa Ana and the weaker northwesterly regime (Regimes 1 and 2) can be triggered by any of the large-scale flow situations. By contrast the stronger northwesterly regime (Regime 3) is associated with instantaneous realizations of the climatological large-scale circulation. It is also important to note that a particular local wind regime may occur without the simultaneous onset of the synoptic conditions that appear to favor it. The origin and maintenance of these local wind regimes are therefore still unclear.

The Santa Ana wind regime is associated with a strong cooling of the Great Basin and the Southern California deserts east of the coastal range (see Fig. 5). The warming in the low-lying coastal area of Southern California associated with Santa Ana winds is likely to be the result of compressional warming of desert air as it descends to the coast. Additional work is required to elucidate the possible dynamic and thermodynamic mechanisms involved in the development of the surface pressure anomalies that generate and maintain the Santa Ana wind regime.

Acknowledgments.
It is a pleasure to thank M. Hughes for running the MM5 model intensively. The authors are grateful to D. Kondrashov for providing the gaussian mixture model clustering code and to G. Plaut for providing the ANAXV software used to compute the k-means classification. This work was supported by NSF Grant ATM00-82131 (SC and MG) and by NSF Grant ATM-0135136 (AH).

References

Hu, H., and W.-T. Liu (2003), Oceanic thermal and biological responses to Santa Ana winds, *Geophys. Res. Lett.*, *30*(11), 1596.

Kaihatu, J.-M., R. Handler, G. Marmorino, and L. Shay (1998), Empirical Orthogonal Function analysis of

ocean surface currents using complex and real-vector methodes, *J. Atmos. Ocean. Techn.*, *15*, 927–941.

Kondrashov, D., K. Ide, and M. Ghil (2004), Weather regimes and preferred transition paths in a three-level quasigeostrophic model, *J. Atmos. Sci.*, *61*(5), 568–587.

Leung, L.-R., Y. Qian, X. Bian, and A. Hunt (2003), Hydroclimate of the Western United States based on observations and regional climate simulation of 1981-2000. Part II: Mesoscale ENSO anomalies., *J. Climate*, *16*(12), 1912–1928.

Lu, R., R.-P. Turco, K. Stolzenbach, S.-K. Friedlander, C. Xiong, L. Schiff, K. Tiefenthaler, and G. Wang (2003), Dry deposition of airborne trace metals on the Los Angeles Basin and adjacent coastal waters, *J. Geophys. Res.*, *108*(D2), 4074–4098.

Ludwig, F., J. Horel, and D. Whiteman (2004), Using EOF analysis to identify important surface wind patterns in mountain valleys, *J. Applied Meteorol.*, *43*(7), 969–983.

Michelangeli, P.-A., R. Vautard, and B. Legras (1995), Weather regimes: recurrence and quasi stationarity, *J. Atmos. Sci.*, *52*, 1237–1256.

Raphael, M.-N. (2003), The Santa Ana winds of California, *Earth Interactions*, *7*, 8.1–8.13.

Robertson, A.-W., and M. Ghil (1999), Large-scale weather regimes and local climate over the Western United States., *J. Climate*, *12*(6), 1796–1813.

Smyth, P., K. Ide, and M. Ghil (1999), Multiple regimes in Northern Hemisphere height fields via mixture model clustering, *J. Atmos. Sci.*, *56*, 3704–3723.

Sommers, W.-T. (1978), LFM forecast variables related to Santa Ana wind occurrences, *Mon. Wea. Rev.*, *106*(9), 1307–1316.

Travisña, A., M. Ortiz-Figuerora, H. Herrera, M.-A. Cosio, and E. Gonzalez (2003), Santa Ana winds and upwelling filaments off Northern Baja California, *Dyn. Atmos. Oceans*, *37*, 113–127.

Westerling, A., D. Cayan, T. Brown, B. Hall, and L. Riddle (2004), Climate, Santa Ana winds and autumn wildfires in Southern California, *Eos Trans AGU*, *85*(31), 289–300.

Winant, C.-D., and C.-E. Dorman (1997), Seasonal patterns of surface wind stress and heat flux over the Southern California Bight, *J. Geophys. Res.*, *102*(C3), 5641–5653.

S. Conil, Department of Atmospheric and Oceanic Sciences, UCLA 405 Hilgard, Los Angeles, CA 90095-1565, USA. (conil@atmos.ucla.edu)

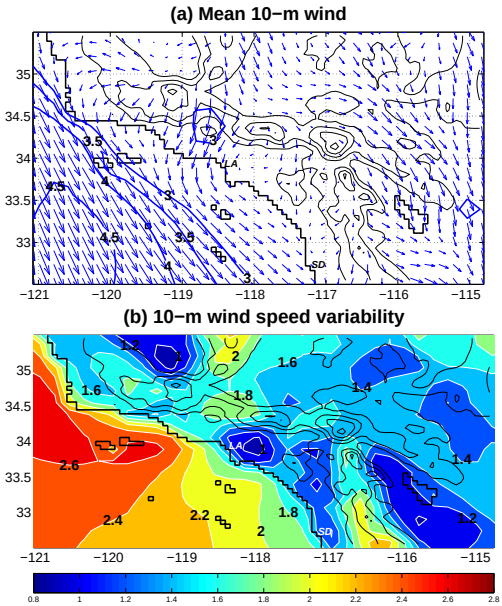

Figure 1. Climatological winter conditions over Southern California. (a) mean wind (vectors) and mean wind speed (blue contours); (b): standard deviation of the wind speed Oct-Mar 1995-2003. Units: ms^{-1}. The topography is shown in black contours (intervals = 500 m). Only every third grid point is shown here for clarity of plotting in displaying the winds.

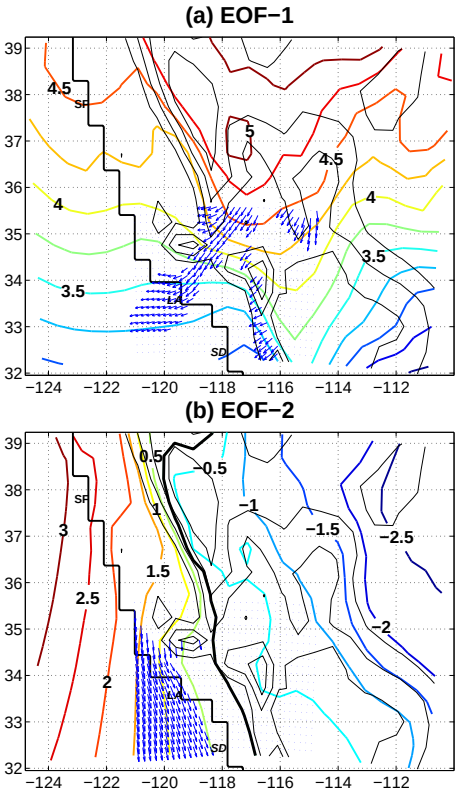

Figure 2. Empirical orthogonal functions (EOFs) of the surface pressure (contours, units: hPa) and wind anomalies (arrows) Oct–Mar 1995–2003; first (a) and second (b) EOF. Units: hPa. Anomalous winds above 2.5 $m.s^{-1}$ are plotted. Topography and plotting conventions as in Fig. 1a.

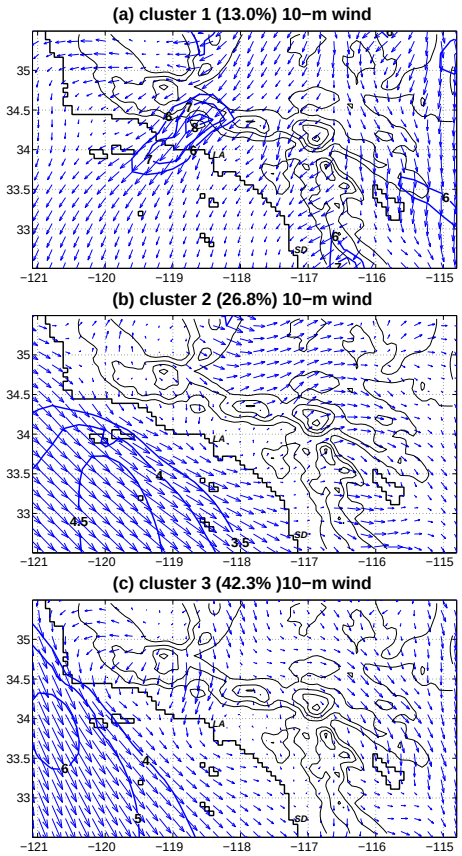

Figure 3. The 3 clusters identified by a mixture model clustering algorithm applied in the subspace spanned by the two leading EOFs of the wind anomalies in South California during the winters 1995–2003. Probability of occurrence indicated in parenthesis. The blue contours show the wind speed (units: ms^{-1}).Conventions for topography and wind vectors as in Fig. 1a.

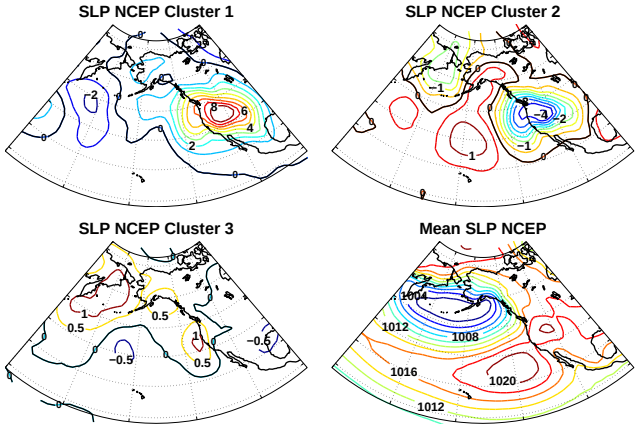

Figure 4. Composites of sea level pressure (SLP) anomalies associated with the 3 wind regimes and mean climatological SLP (NCEP reanalysis Oct–Mar 1995–2003). Units: hPa.

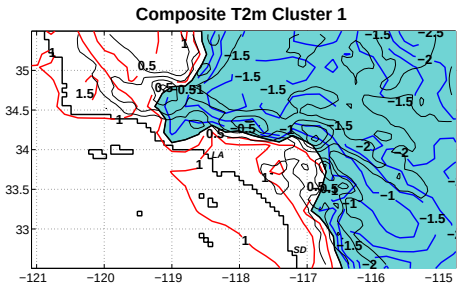

Figure 5. Composite of the 2-m temperature anomalies associated with the Santa Ana wind regime. Units: ^{o}C. Topography shown as in Fig. 1a.